

Article

Preparation of Ferrotitanium Using Ilmenite with Different Reduction Degrees

Zixian Gao ¹, Gongjin Cheng ^{1,2}, He Yang ^{1,2}, Xiangxin Xue ^{1,2,*} and Jongchol Ri ¹¹ School of Metallurgy, Northeastern University, Shenyang 110819, China² Liaoning Key Laboratory of Recycling Science for Metallurgical Resources, Shenyang 110819, China

* Correspondence: xuexx@mail.neu.edu.cn; Tel.: +86-024-8368-7719; Fax: +86-024-2390-6316

Received: 2 August 2019; Accepted: 27 August 2019; Published: 2 September 2019



Abstract: The effect of ilmenite with different reduction degrees on the production of ferrotitanium, using a self-propagation high-temperature synthesis method with aluminum as the reducing agent, was investigated. Increasing the degree of reduction not only contributed to lower consumption of aluminum, but also lowered the oxygen content and improved the grades of titanium and iron in the ferrotitanium. The aluminum content of the ferrotitanium increased with an increase in the extent of reduction of ilmenite, so the Al_2O_3 content formed in the slag decreased with the constant addition of CaO and CaF_2 to the Al powder. This decreased relatively the content of high-melting-point $\text{CaAl}_{12}\text{O}_{19}$ and increased the contents of low-melting-point CaAl_2O_4 and CaF_2 in the slag, thereby promoting the separation of ferrotitanium and slag. Improving the reduction degree of ilmenite is beneficial to the preparation of ferrotitanium.

Keywords: ilmenite; reduction; self-propagation high-temperature synthesis; ferrotitanium; slag

1. Introduction

Ilmenite (FeTiO_3), a titanium-bearing ore, is abundant and economical [1,2], and is essential for the production of metallic titanium [3] and titanium-containing materials [2,4–17]. Ferrotitanium is used as a steelmaking additive [18–20] and as a raw material for the production of ferrosilicotitanium [21,22]. There are three main methods for the production of ferrotitanium: re-melting, molten salt electrolysis [4–6,19], and the aluminothermic method [12,16].

The aluminothermic method predominates for the production of ferrotitanium in China, owing to the lack of titanium scrap and the low efficiency of molten salt electrolysis. Researchers have reported the effect of the ratio of ilmenite to rutile, Al, and KClO_4 on the preparation of ferrotitanium by the aluminothermic method. With an increase in the ratio of ilmenite to rutile, the Ti content of ferrotitanium and the density of slag increased, and metal inclusions in the slag decreased [16,23]. The titanium concentration in the ferrotitanium decreased as the ferrotitanium yield in the refining process decreased [16]. The oxygen content was positively correlated with the titanium content. It was possible to decrease the oxygen content to 4–5% in refined ferrotitanium containing 55–65% Ti based on the main phase component, $\text{Ti}_4\text{Fe}_2\text{O}$. An investigation of the effects of Al and KClO_4 in the self-propagating high-temperature synthesis (SHS) of ferrotitanium found that coarse Al powders were able to decrease burning velocity and material loss caused by sputtering and increase the yield of the target material to ingot. An increase in Al and KClO_4 contents increased material loss caused by sputtering and decreased the yield of target material to ingot, when the Al and KClO_4 contents exceeded 20 mass% and 7 mass%, respectively. It was also reported that an increase of slag volume was detrimental to the recovery of titanium and increased consumption of aluminum [24]. Thus, reducing the slag volume is considered a target for future improved production of ferrotitanium.

Most research has focused on natural ilmenite as the raw material for the preparation of ferrotitanium. Improving the degree of reduction of ilmenite not only decreases the aluminum consumption, but also reduces the slag volume. In this work, the effect of the degree of ilmenite reduction on the preparation of ferrotitanium was investigated by analysis of chemical compositions, phase transitions, and morphologies of the ferrotitanium and slag.

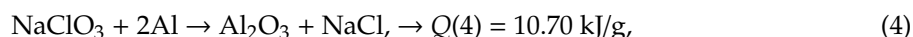
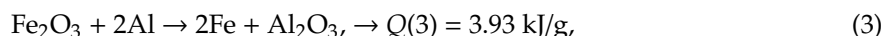
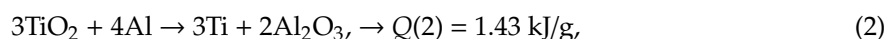
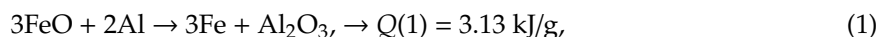
2. Experimental

2.1. Materials

Ilmenite was obtained from Liaoning, China. It comprised 26.85 mass% FeO, 19.48 mass% Fe₂O₃, and 44.44 mass% TiO₂. Ilmenite pellets were prepared by mixing ilmenite and additional 2 mass% bentonite as a binder in a disc pelletizer, and then roasted in a muffle furnace at 1200 °C for 2 h in the presence of 2.5 L/min air. Ilmenites of varying reduction degrees were obtained by combinations of natural and reduced ilmenite. Reduced ilmenite was obtained by reducing the pellets for 0, 30, and 240 min at 1100 °C in a carbon monoxide atmosphere, which was calculated on the basis of reduction formula of iron oxides [25]. The reduction degrees was 0%, 43%, and 75%, respectively. The reduction degree of natural ilmenite was 11%, calculated based on oxidized ilmenite. Natural ilmenite and reduced pellets were crushed to a powder of less than 75 µm in diameter to provide the feed material for SHS. TiO₂ (99%, <75 µm), Al (98%, <75 µm), CaO (99%, <75 µm), CaF₂ (99%, <75 µm), and NaClO₃ (99%, <75 µm) were all of chemical-reagent grade.

2.2. Theoretical Calculation

The main reactions of the SHS process are the reduction of iron oxide and titanium dioxide by aluminum powder to metal, as shown in Equations (1) to (3). NaClO₃ is an exothermal agent that reacts with the aluminum powder to provide heat of 2.86 kJ/g of the reacting substances to ensure that the SHS reaction takes place spontaneously and that the ferrotitanium and slag are well separated, as presented in Equation (4). The heat released per unit mass of reacting substance was calculated by Equation (5).



$$Q_{(average)} = \frac{m_1Q(1) + m_2Q(2) + m_3Q(3) + m_4Q(4)}{m_{total}}. \quad (5)$$

In Equation (5), m_1 to m_4 are the combined masses of FeO, TiO₂, Fe₂O₃, and NaClO₃ and aluminum that participate in Equations (1) to (4), respectively.

2.3. Experimental Methods

Except for the aluminum powder, the raw materials were dried in an oven at 110 °C for 12 h. The materials ratios are presented in Table 1. In this work, element Fe originated from the ilmenite and Ti from the ilmenite and TiO₂. CaO and CaF₂ were added at 20 mass% and 10 mass% of the aluminum powder, respectively. After burdening, the compositions were mixed for 2 h in a blender, and then 750 g of the mixed material was placed in a graphite crucible lined with magnesia sand. The SHS reactions were initiated by employing upper ignition. After cooling to room temperature, a ferrotitanium block was obtained after removing the slag.

Table 1. Materials ratios in the experiment.

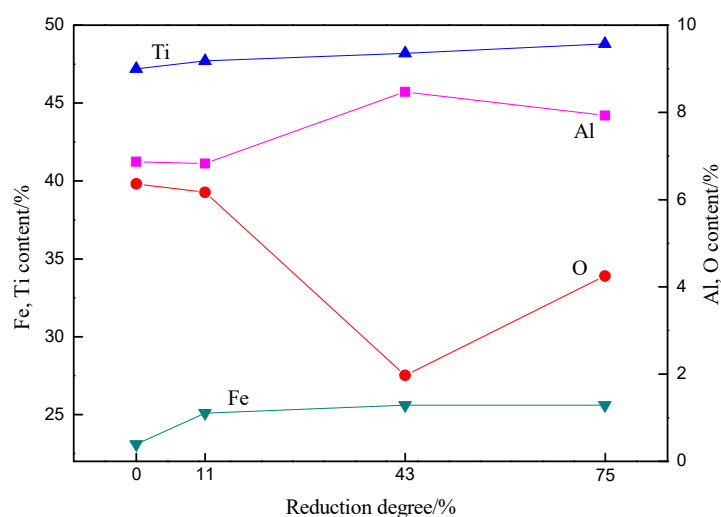
Reduction Degree/%	Ilmenite/g	TiO ₂ /g	Al/g	NaClO ₃ /g	CaO/g	CaF ₂ /g
0	500	822	652	217	130	65
11	482	822	643	229	129	64
43	471	822	633	244	127	63
75	450	822	619	264	124	62

The composition of the ilmenite was measured by chemical analysis and X-ray fluorescence (XRF; ZSXPrimus-II, Rigaku, Tokyo, Japan). After the SHS reactions were complete, the ferrotitanium alloy was crushed to a powder of less than 75 μm to measure the Fe, Ti, and Al contents. O content was measured using two small pieces of the alloy with a mass of about 0.1 g. Fe, Ti, Al, and O contents were analyzed by inductively coupled plasma optical emission spectrometry (ICP–OES; Optima 8300DV, PerkinElmer, Waltham, MA, USA) and by oxygen/nitrogen/hydrogen elemental analysis (ONH836, LECO, USA). X-ray diffractometry (XRD; X’Pert Pro, PANalytical, Almelo, The Netherlands) was used to determine the phases present in the ferrotitanium and slag. Scanning electron microscopy linked to energy-dispersive spectroscopy (SEM–EDS; Ultra Plus, Carl Zeiss, Oberkochen, Germany) was applied to observe the microstructure and determine the chemical compositions of different phases of ferrotitanium and slag. Prior to observation, a cross-section of ferrotitanium was etched for 15 s using an aqueous solution containing 2 vol.% HF and 4 vol.% HNO₃.

3. Results

3.1. Chemical Composition of Ferrotitanium

The chemical composition of ferrotitanium is presented in Figure 1. The contents of Fe and Ti increase with increasing reduction degrees of ilmenite. The Al content has an increasing trend, while O shows the opposite outcome.

**Figure 1.** Effect of reduction degrees of ilmenite on the chemical composition of ferrotitanium.

3.2. Phase Transitions

From the XRD patterns, shown in Figure 2, it is found that the ferrotitanium slags comprise $\text{CaAl}_{12}\text{O}_{19}$, CaAl_2O_4 , Al_2O_3 , FeO , CaTiO_3 , TiO , and CaF_2 . FeO diffraction peaks only occur in the slags formed from ilmenites with 0% and 11% reduction, as shown in Figure 2a,b, respectively. When the extent of reduction of ilmenite increases to 11%, CaAl_2O_4 and CaF_2 peaks are found in XRD analysis of the slag. Figure 3 shows the phases of ferrotitanium as a function of different reduction degrees of ilmenite. $\text{Ti}_4\text{Fe}_2\text{O}$, Ti_2O , and Al_2O_3 are the main oxygen-bearing phases. All XRD patterns

of ferrotitanium show the presence of $\text{Ti}_4\text{Fe}_2\text{O}$, AlTi_3 , $\text{Al}_3\text{Ti}_{0.75}\text{Fe}_{0.25}$, Ti_2O , and FeTi phases. Al_2O_3 diffraction peaks are found in ferrotitanium produced from unreduced ilmenite, while Al_3Ti peaks only occur in ferrotitanium produced from ilmenite with 75% reduction degree. Reduction of SiO_2 is also enhanced by increasing the degree of reduction; hence, SiTi is found in ferrotitanium prepared from ilmenites with 43% and 75% reduction degree, as shown in Figure 3c,d, respectively.

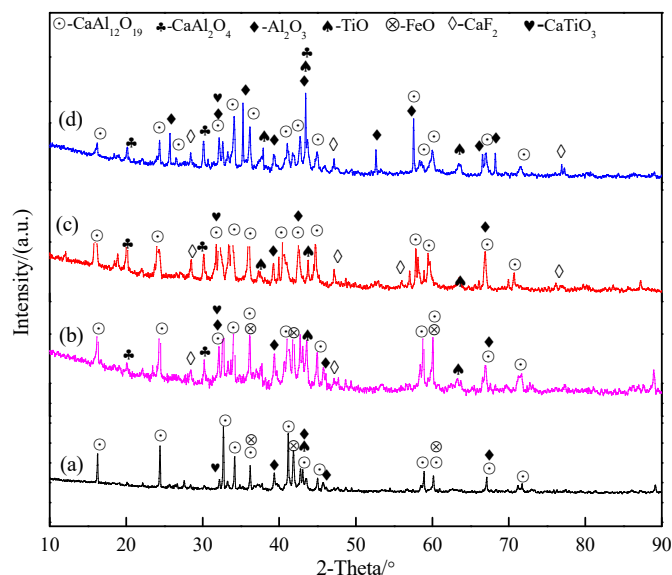


Figure 2. X-ray diffraction patterns of slags formed from ilmenites with different reduction degrees. (a) 0%, (b) 11%, (c) 43%, and (d) 75%.

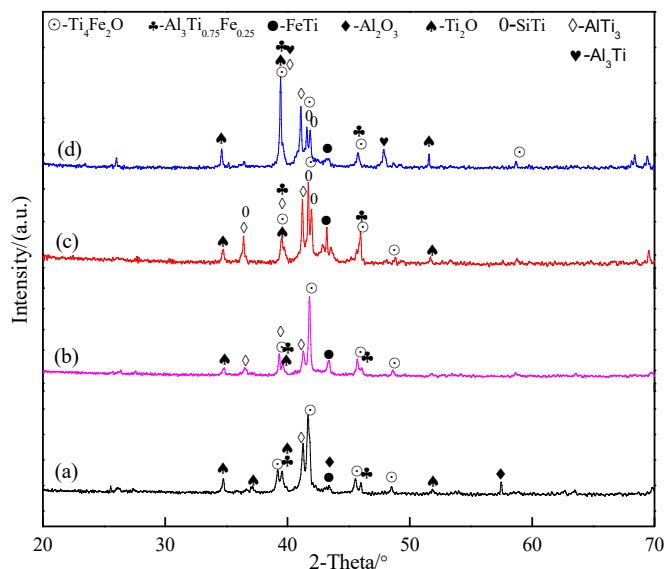


Figure 3. X-ray diffraction patterns of ferrotitanium produced from ilmenites with different reduction degrees. (a) 0%, (b) 11%, (c) 43%, and (d) 75%.

3.3. Morphology of Ferrotitanium and Slag

Figure 4 shows the macroscopic morphology of ferrotitanium produced by ilmenite with different reduction degrees. Ferrotitanium produced by ilmenite with a low extent of reduction is porous and difficult to separate from the slag, owing to the ferrotitanium and slag embedding within each other, as shown in Figure 4a,b. Figure 4c,d show that the ferrotitanium (light-gold color) produced from more highly reduced ilmenite is dense, and there is excellent separation between the slag and ferrotitanium.

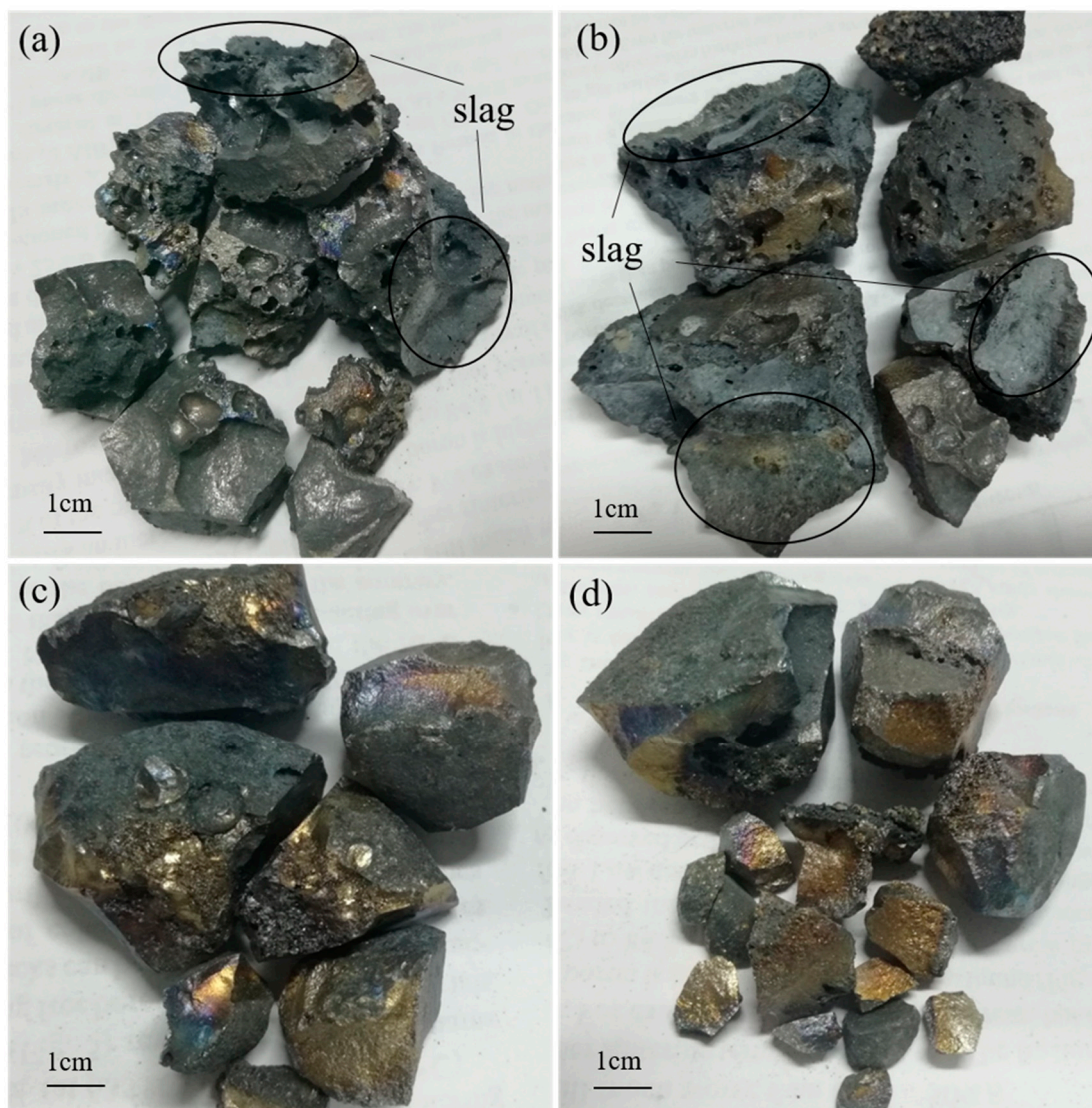


Figure 4. Macroscopic morphology of ferrotitanium produced from ilmenites with different reduction degrees. (a) 0%, (b) 11%, (c) 43%, and (d) 75%.

Microstructures of the slags, obtained from SEM–EDS analysis, are presented in Figures 5 and 6. Figure 6 is an enlargement of the white frames in Figure 5. From Table 2, there is no doubt that points A and J comprise complex phases composed of Ca, Al, Ti, O, and F; that points F and G are alloy phases of Ti–Si and Fe–Ti–Si, respectively; and that B, D, H, and I are TiO, $\text{CaAl}_{12}\text{O}_{19}$, Al_2O_3 , and CaAl_2O_4 , respectively. Points C and K assay as $2(\text{Ca,Ti})\text{O}\cdot\text{Al}_2\text{O}_3$ and point E comprises $(\text{Ca,Ti})\text{O}\cdot 6\text{Al}_2\text{O}_3$. The $\text{CaAl}_{12}\text{O}_{19}$ phases are acicular (Figure 5a) and the TiO phases in the slag are approximately spherical (Figure 6). The TiO phases are enriched in $\text{CaAl}_{12}\text{O}_{19}$ phases or their boundaries, as shown in Figure 5a,b. Some alloy phases are enclosed in slag, as presented in Figure 5b,d. Considering the phase transitions shown in Figure 2 and the microstructures of Figure 5, it is concluded that the acicular $\text{CaAl}_{12}\text{O}_{19}$ content decreases and the Al_2O_3 and CaAl_2O_4 contents increase with an increase in the degree of reduction of ilmenite.

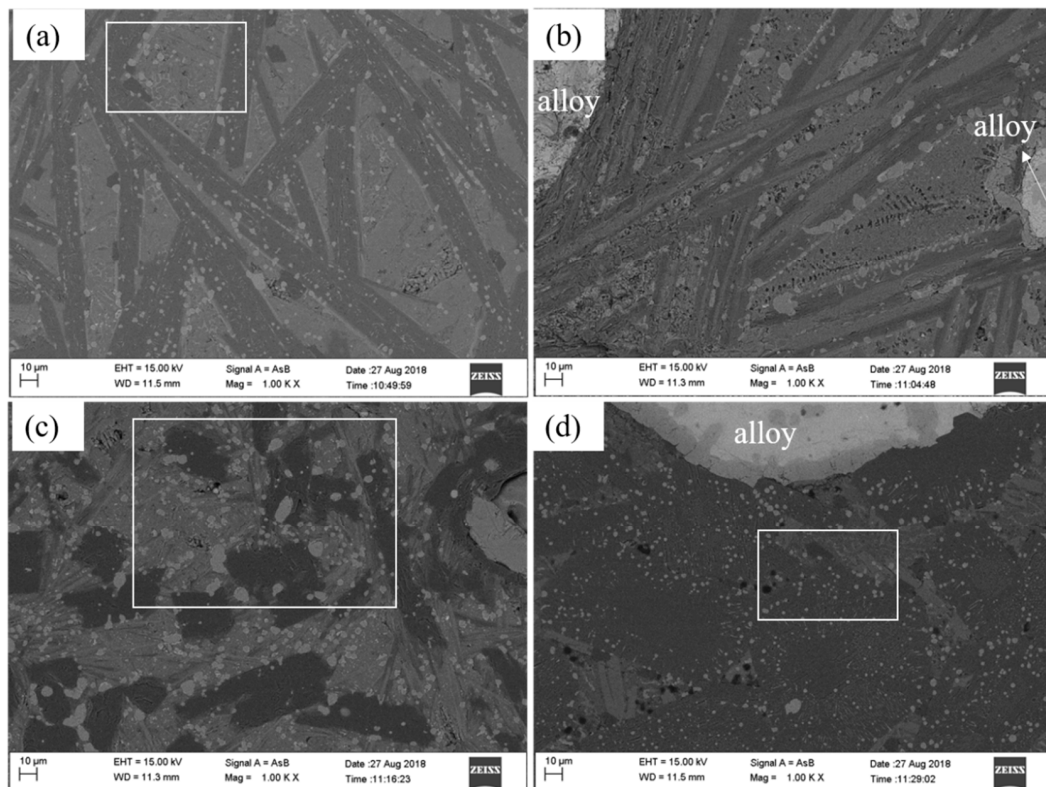


Figure 5. Microstructures of slag produced from ilmenites with different reduction degrees. (a) 0%, (b) 11%, (c) 43%, and (d) 75%.

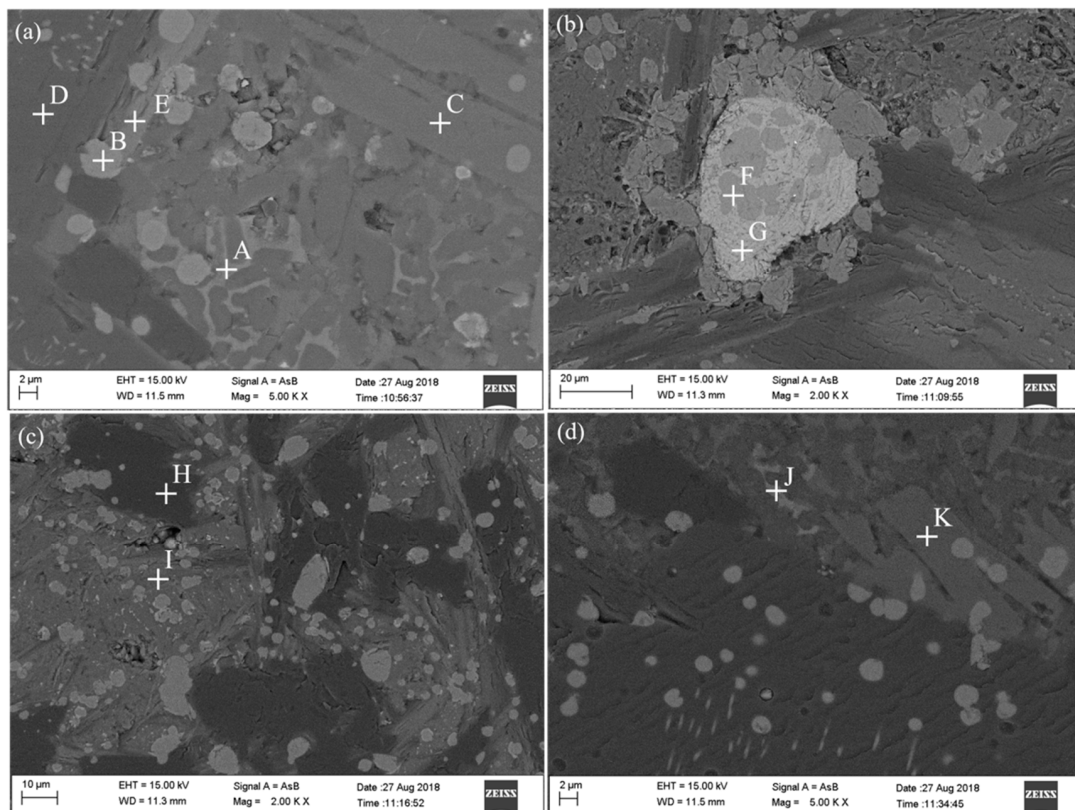


Figure 6. Microstructures of slag produced from ilmenites with different reduction degrees, shown at higher magnification. (a) 0%, (b) 11%, (c) 43%, and (d) 75%.

Table 2. The atomic proportions of phases in Figure 6, %.

Point	Fe	Ti	Al	O	Ca	Si	F	Mg	Na
A		12.75	11.48	57.00	15.67	0.13	2.39	0.32	0.26
B		41.44	2.47	54.43	0.48			1.19	
C		15.30	20.45	57.46	5.88			0.91	
D		3.22	36.57	55.97	3.00			1.23	
E		3.04	32.51	60.75	0.31			2.76	0.65
F	4.12	55.26		11.54		28.60			
G	30.60	38.36	1.28	10.84		13.57			
H		0.88	43.69	55.43					
I		2.33	28.46	55.59	13.62				
J		15.26	6.70	56.26	16.81		4.48		0.48
K		13.66	22.90	56.13	6.24		1.06		

Microstructures of ferrotitanium are presented in Figure 7. Three main phases are apparent from Figure 7a,b. As given in Table 3, the color of the phase changes from light to dark gray with an increase of Ti content. From analysis of the relative atomic proportions, the light-gray phases L and O are found to be the oxygen-bearing phase Ti_4Fe_2O , the intermediate-gray phases N and Q are oxygen-bearing Ti-rich phases, and the dark-gray phases M and P are Ti_2O . In Figure 7c, point T comprises Ti_4Fe_2O , and R and S are oxygen-free alloy phases. In ferrotitanium, Ti_4Fe_2O is the matrix within which Ti-rich alloy phases containing Ti_2O are distributed. Ferrotitanium prepared from unreduced ilmenite contains more Ti_2O than that from 75% reduced ilmenite.

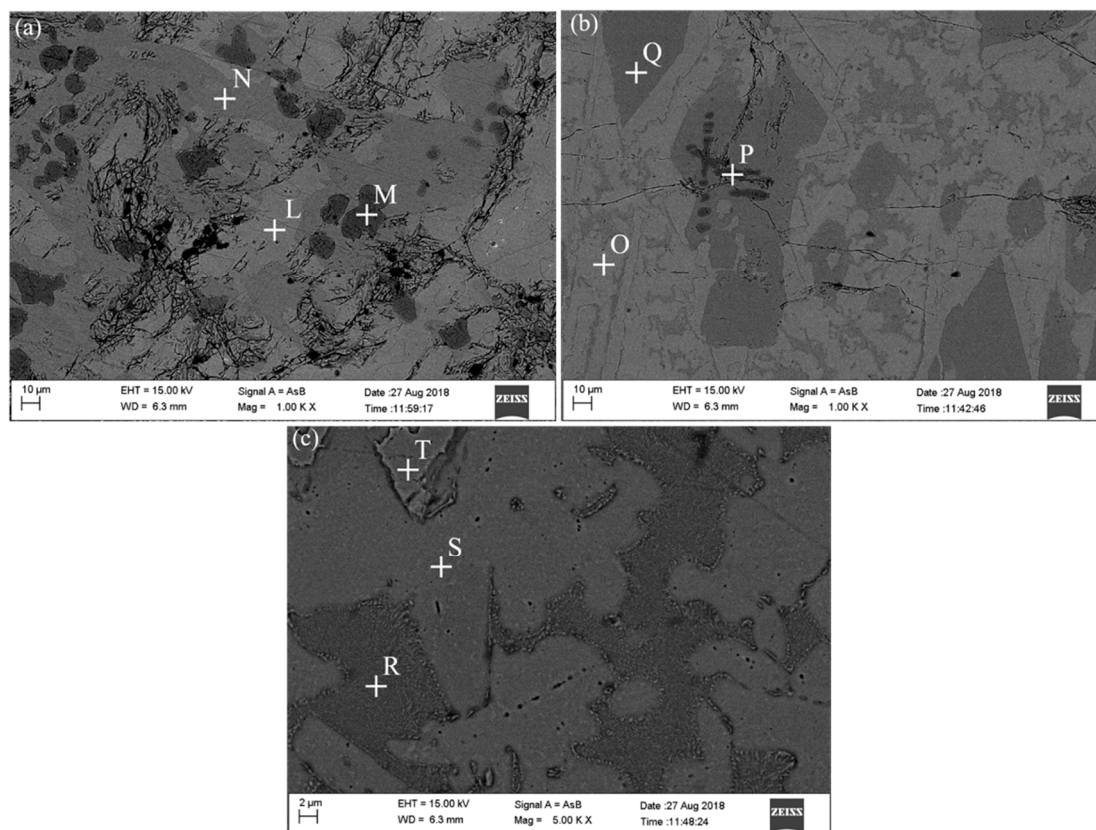


Figure 7. Microstructures of ferrotitanium produced from ilmenites with different reduction degrees. (a) 0%, (b) 75%, and (c) 75%.

Table 3. The atomic proportions of phases in Figure 7, %.

Point	Fe	Ti	Al	O	Si
L	21.34	46.83	17.84	11.29	2.70
M		64.17		35.64	
N	12.31	55.35	5.62	22.87	3.85
O	24.53	46.77	8.08	15.35	4.82
P		62.48		37.52	
Q	11.44	54.14	6.02	20.70	3.68
R	20.16	56.20	19.15		4.50
S	33.87	41.41	20.17		4.55
T	25.59	46.48	8.00	14.61	5.33

4. Discussion

As mentioned above, an increase in the extent of reduction of ilmenite is helpful to improve the grades of iron and titanium in ferrotitanium and can also decrease its oxygen content. Although the aluminum content shows an increasing trend with increasing ilmenite reduction, the product still meets the Chinese specifications for FeTi50B (GB/T 3282-2012). With increasing the extent of reduction of ilmenite, the amount of iron oxide in the SHS raw materials is lowered. The remaining iron oxide is more easily reduced to metallic Fe with increasing the degree of reduction, so there is no evidence of FeO in the slag when the reduction exceeds 43%. The iron grade of ferrotitanium increases with the extent of reduction. TiO is an intermediate product in the reduction of titanium oxide. This is a basic oxide and is able to combine with Al_2O_3 to form composite compounds [26], which is the main reason for the formation of TiO, $2(\text{Ca,Ti})\text{O}\cdot\text{Al}_2\text{O}_3$, and $(\text{Ca,Ti})\text{O}\cdot 6\text{Al}_2\text{O}_3$ in the slag. Owing to incomplete reduction of TiO_2 , the Al present as a reductant for titanium oxide has a surplus in the SHS process. With increasing ilmenite reduction degrees, the ratio of residual aluminum to aluminum as the reductant for iron oxide and TiO_2 gradually increases. Residual aluminum melts in the ferrotitanium as an alloy element. The high Al content leads to the formation of Al_3Ti in ferrotitanium, as shown in Figure 3d. Furthermore, an increase of Al content enhances its activity in ferrotitanium, which promotes the reduction of Ti_2O in ferrotitanium and TiO in slag. The fact that the Al and O contents show opposing trends in the ferrotitanium with varying degrees of ilmenite reduction also proves this point: thus, compared with Figure 7a, there is less unreduced Ti_2O in Figure 7b. This is the main reason for the decrease of the O content in ferrotitanium. When the reduction degree is above 43%, the O content increases slightly as a result of the increase of $\text{Ti}_4\text{Fe}_2\text{O}$ with the increase of Ti content, as shown in Figure 3d. In addition, the increase of the residual aluminum also can promote the reduction of silica, hence the new phase, SiTi, is generated in the ferrotitanium produced by the high extent of reduction of ilmenite, as revealed in Figure 3c,d.

Metallic Ti melted in metallic Fe during the reduction of TiO_2 . This can reduce its volatilization and facilitate the reduction of TiO_2 because of the decrease in Ti activity [23]. Therefore, volatilization of Ti decreased and reduction of TiO_2 is enhanced with increasing iron grade in the ferrotitanium. Its Ti content increased with increasing ilmenite reduction degree.

With an increase of Al content in the ferrotitanium, Al_2O_3 formed in the SHS process decreases with a constant addition ratio of CaO and CaF_2 to Al. Thus, there is a relative increase in the CaF_2 and CaO contents in the slag with increasing ilmenite reduction. Owing to the use of the same ratio of CaO to CaF_2 , Figure 8 shows that point A moves away from the direction of Al_2O_3 along the blue line in the Al_2O_3 –CaO– CaF_2 ternary phase diagram drawn by FactSage 7.0; hence, the melting point of the slag decreases with an increase in reduction. The same conclusion also can be obtained from slag phases. An increase of CaO caused a decrease in the $\text{CaAl}_{12}\text{O}_{19}$ content and increase in CaAl_2O_4 , as shown in Figures 2 and 5. As the contents of low-melting-point CaF_2 and CaAl_2O_4 increased, slag is more easily separated from the ferrotitanium. An increase in the degree of reduction of ilmenite thus promotes the separation of ferrotitanium and slag.

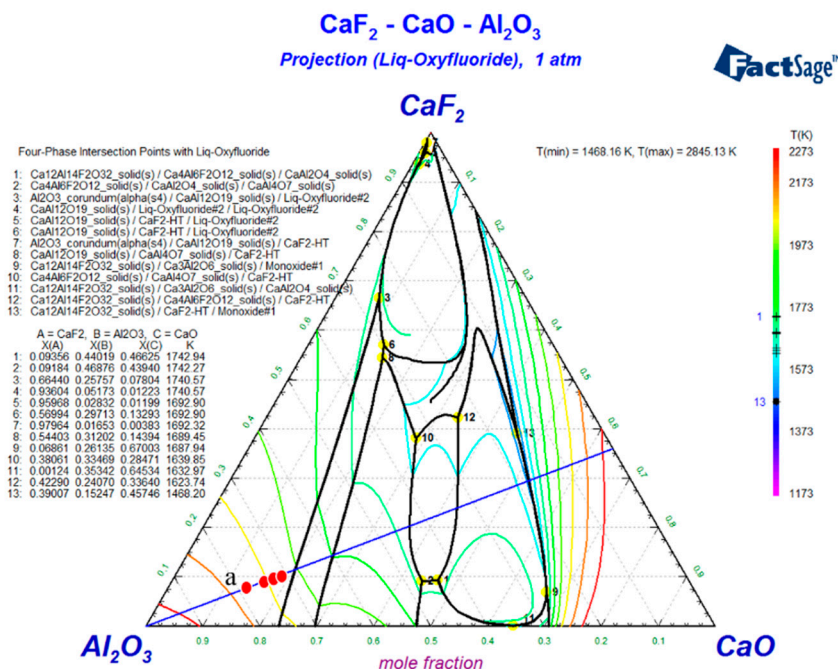


Figure 8. Ternary phase diagram of Al₂O₃-CaO-CaF₂.

5. Conclusions

This work investigated the effect of the reduction degree of ilmenite on the chemical and phase characteristics of the resulting ferrotitanium and slag produced by the SHS aluminothermic process. Improving the reduction not only decreases the consumption of aluminum and the amount of slag generated in the preparation of ferrotitanium, but also reduces the oxygen content and improves the grades of titanium and iron. The aluminum content of the ferrotitanium increases with increasing ilmenite reduction degree, so the Al₂O₃ content formed in the SHS process decreases with addition of a constant ratio of CaO and CaF₂ to Al in the raw materials. Relatively, the CaF₂ and CaO contents increases in the slag. This decreases the content of high-melting-point CaAl₁₂O₁₉ in the slag and increases the contents of low-melting-point CaAl₂O₄ and CaF₂, thereby promoting the separation of ferrotitanium and slag.

Author Contributions: Conceptualization, X.X. and Z.G.; validation, Z.G., G.C. and H.Y.; formal analysis, Z.G. and G.C.; investigation, Z.G. and X.X.; resources, H.Y.; data curation, Z.G.; writing—original draft preparation, Z.G.; writing—review and editing, X.X., Z.G., G.C. and J.R.; visualization, G.C., J.R. and H.Y.; supervision, X.X. and Z.G.; project administration, X.X.

Funding: This research was funded by National Natural Science Foundation of China, grant number 51674084.

Conflicts of Interest: The authors declare that they have no conflict of interest.

References

- Chen, M.; Tang, A.-T.; Xiao, X. Effect of milling time on carbothermic reduction of ilmenite. *Trans. Nonferrous Met. Soc. China* **2015**, *25*, 4201–4206. [\[CrossRef\]](#)
- Panigrahi, M.; Shibata, E.; Iizuka, A.; Nakamura, T. Production of Fe-Ti alloy from mixed ilmenite and titanium dioxide by direct electrochemical reduction in molten calcium chloride. *Electrochim. Acta* **2013**, *93*, 143–151. [\[CrossRef\]](#)
- Panigrahi, M.; Paramguru, R.K.; Gupta, R.C.; Shibata, E.; Nakamura, T. An overview of production of titanium and an attempt to titanium production with ferro-titanium. *High Temp. Mater. Processes* **2010**, *9*, 495–514. [\[CrossRef\]](#)

4. Xiong, L.; Hua, Y.; Xu, C.; Li, J.; Li, Y.; Zhang, Q.; Zhou, Z.; Zhang, Y.; Ru, J. Effect of CaO addition on preparation of ferrotitanium from ilmenite by electrochemical reduction in CaCl₂-NaCl molten salt. *J. Alloys Compd.* **2016**, *676*, 383–389. [\[CrossRef\]](#)
5. Qi, C.-c.; Hua, Y.-x.; Chen, K.-h.; Jie, Y.-f.; Zhou, Z.-r.; Ru, J.-j.; Xiong, L.; Gong, K. Preparation of ferrotitanium alloy from ilmenite by electrochemical reduction in chloride molten salts. *JOM* **2015**, *68*, 668–674. [\[CrossRef\]](#)
6. Zhou, Z.; Hua, Y.; Xu, C.; Li, J.; Li, Y.; Gong, K.; Ru, J.; Xiong, L. Preparation of Ferrotitanium from Ilmenite by Electrolysis-Assisted Calciothermic Reduction in CaCl₂-NaCl Molten Salt. *JOM* **2015**, *68*, 532–539. [\[CrossRef\]](#)
7. Lv, W.; Lv, X.; Zhang, Y.; Li, S.; Tang, K.; Song, B. Isothermal oxidation kinetics of ilmenite concentrate powder from Panzhihua in air. *Powder Technol.* **2017**, *320*, 239–248. [\[CrossRef\]](#)
8. Li, Z.; Wang, Z.; Li, G. Preparation of nano-titanium dioxide from ilmenite using sulfuric acid-decomposition by liquid phase method. *Powder Technol.* **2016**, *287*, 256–263. [\[CrossRef\]](#)
9. Middlemas, S.; Fang, Z.Z.; Fan, P. Life cycle assessment comparison of emerging and traditional Titanium dioxide manufacturing processes. *J. Cleaner Prod.* **2015**, *89*, 137–147. [\[CrossRef\]](#)
10. Gou, H.-P.; Zhang, G.-H.; Chou, K.-C. Influence of pre-oxidation on carbothermic reduction process of ilmenite concentrate. *ISIJ Int.* **2015**, *55*, 928–933. [\[CrossRef\]](#)
11. Khoshhal, R.; Soltanieh, M.; Boutorabi, M.A. Formation mechanism and synthesis of Fe–TiC/Al₂O₃ composite by ilmenite, aluminum and graphite. *Int. J. Refract. Met. Hard Mater* **2014**, *45*, 53–57. [\[CrossRef\]](#)
12. Azizov, S.T.; Kachin, A.R.; Loryan, V.E.; Borovinskaya, I.P.; Mnatsakanyan, A.S. Aluminothermic SHS of ferrotitanium from ilmenite: Influence of Al and KClO₄ content of green composition. *Int. J. Self Propag. High Temp. Synth.* **2014**, *23*, 161–164. [\[CrossRef\]](#)
13. Akhgar, B.; Pazouki, M.; Ranjbar, M.; Hosseinnia, A.; Salarian, R. Application of Taguchi method for optimization of synthetic rutile nano powder preparation from ilmenite concentrate. *Chem. Eng. Res. Des.* **2012**, *90*, 220–228. [\[CrossRef\]](#)
14. Wu, L.; Li, X.; Wang, Z.; Guo, H.; Wang, X.; Wu, F.; Fang, J.; Wang, Z.; Li, L. A novel process for producing synthetic rutile and LiFePO₄ cathode material from ilmenite. *J. Alloys Compd.* **2010**, *506*, 271–278. [\[CrossRef\]](#)
15. Wang, X.; Li, X.; Wang, Z.; Wu, L.; Yue, P.; Guo, H.; Wu, F.; Ma, T. Preparation and characterization of Li₄Ti₅O₁₂ from ilmenite. *Powder Technol.* **2010**, *204*, 198–202. [\[CrossRef\]](#)
16. Chumarev, V.M.; Dubrovskii, A.Y.; Pazdnikov, I.P.; Shurygin, Y.Y.; Sel'menskikh, N.I. Technological possibilities of manufacturing high-grade ferrotitanium from crude ore. *Russ. Metall.* **2009**, *2008*, 459–463. [\[CrossRef\]](#)
17. Lasheen, T.A. Soda ash roasting of titania slag product from Rosetta ilmenite. *Hydrometallurgy* **2008**, *93*, 124–128. [\[CrossRef\]](#)
18. Yang, W.; Zhang, Y.; Zhang, L.-f.; Duan, H.-j.; Wang, L. Population evolution of oxide inclusions in ti-stabilized ultra-low carbon steels after deoxidation. *J. Iron. Steel Res. Int.* **2015**, *22*, 1069–1077. [\[CrossRef\]](#)
19. Pande, M.M.; Guo, M.; Blanpain, B. Inclusion formation and interfacial reactions between FeTi alloys and liquid steel at an early stage. *ISIJ Int.* **2013**, *53*, 629–638. [\[CrossRef\]](#)
20. Chen, L. Study on the effects of Ti micro-addition on the characteristics of MnS inclusions in rail steel. *Ironmaking Steelmaking* **2017**, *46*, 508–512. [\[CrossRef\]](#)
21. Shatokhin, I.M.; Shaimardanov, K.R.; Bigeev, V.A.; Ziatdinov, M.K.; Shchegoleva, E.A.; Manashev, I.R. Production of ferrosilicotitanium for smelting pipe steels. *Metallurgist* **2016**, *60*, 524–529. [\[CrossRef\]](#)
22. Shaimardanov, K.R.; Shatokhin, I.M.; Ziatdinov, M.K. Production and use of ferrosilicotitanium produced by self-propagating high-temperature synthesis. *Steel Transl.* **2014**, *44*, 215–220. [\[CrossRef\]](#)
23. Jiang, X. Study on Preparation of High Titanium Ferroalloy by Thermite Method and Its Deoxidizing Performance in Molten Steel. Master's Thesis, Northeastern University, Shenyang, China, June 2012.
24. Misra, S.B.; Kamble, A.; Yadav, S.; Ranganathan, S. Influence of charge segregation on specific aluminium consumption in production of ferro-titanium. *Can. Metall. Q.* **2014**, *54*, 101–109. [\[CrossRef\]](#)
25. Gao, Z.; Cheng, G.; Xue, X.; Yang, H.; Duan, P. Property investigations of low-grade vanadium-titanium magnetite pellets with different MgO contents. *Steel Res. Int.* **2018**, *89*, 1700543. [\[CrossRef\]](#)
26. Liu, M.Y.; Xiao, X.H. Development of 65%~75% high grade ferrotitanium with material rutile. *Ferroalloys* **2001**, *158*, 15.

